Available online at www.sciencedirect.com
SCIENCE DIRECT
Spectrochimica Acta Part A 63 (2006) 213–219
SPECTROCHIMICA ACTA PART A
www.elsevier.com/locate/saa

Synthesis, structure, infrared and fluorescence spectra of new rare earth complexes with 6-hydroxy chromone-3-carbaldehyde benzoyl hydrazone

Bao-Dui Wang, Zheng-Yin Yang *, Ding-Wa Zhang, Yan Wang

College of Chemistry and Chemical Engineering and State Key Laboratory of Applied Organic Chemistry, Lanzhou University, Lanzhou 730000, PR China

Received 25 February 2005; received in revised form 30 April 2005; accepted 10 May 2005

Abstract

A novel 6-hydroxy chromone-3-carbaldehyde benzoyl hydrazone ligand and its four complexes, $[LnL_2(NO_3)_2]NO_3$ [Ln = Eu(**1**), Sm(**2**), Tb(**3**), Dy(**4**)], were synthesized. The complexes were characterized by the elemental analyses, molar conductivity and IR spectra. The crystal and molecular structure of Sm(III) complex was determined by single-crystal X-ray diffraction: crystallized in the triclinic system, space group *P*-1, $Z = 1$, $a = 11.037(4)$ Å, $b = 14.770(5)$ Å, $c = 15.032(7)$ Å, $\alpha = 60.583(4)$, $\beta = 75.528(7)$, $\gamma = 88.999(4)$, R1 = 0.0349. The fluorescence properties of complexes in the solid state and in the organic solvent were studied in detail, respectively. Under the excitation of ultraviolet light, strong red fluorescence of solid europium complex was observed. But the green fluorescence of solid terbium complex was not observed. These observations show that the ligand favor energy transfers to the emitting energy level of Eu^{3+}. Some factors that influence the fluorescent intensity were also discussed.

Keywords: Synthesis; Complexes; X-ray structure; Fluorescence properties; 6-Hydroxy chromone-3-carbaldehyde benzoyl hydrazone

1. Introduction

Because they have long fluorescence lifetimes and their excited states have strong fluorescence emission, europium (III) and terbium(III) have extensive applications in biological medicine, especially in the fluorescence imagery cancer radiation treatment [1], fluorescence mark, and fluorescence analysis [2].

The bioactivity and magnetic performance of Schiff base and their complexes with rare earth ions have been studied extensively. However, their fluorescence properties have rarely been studied due to their low luminescence [3,4]. So far, chemists have realized that it is essential to design appropriate ligands to optimize the luminescence properties of lanthanide ions by facilitating the well-known light conversion process, which show to be efficient ligand-to-metal energy-transfer process (antenna effect). Recently, we have designed a series of Schiff base, which can enhance their luminescence by providing proper conjugate absorption groups for suitable energy transfer, and be used as a luminescent device. In the present work, a new and doubly functionalized Schiff-base ligand, 6-hydroxy chromone-3-carbaldehyde benzoyl hydrazone has been synthesized, and the fluorescence properties of europium and terbium complexes with the new ligand have been studied. The results show that the Eu(III) with the ligand can emit intrinsic spectrum of Eu(III) under excitation of ultraviolet light, and that the organic solvent can affect the fluorescence characteristics of the Eu(III) complex.

2. Experimental

2.1. Materials

Acetic anhydride, benzoyl hydrazine, and hydroquinone were produced in China. All material and solvents employed in this study were analytical reagents. Absolute ethanol was

* Corresponding author. Tel.: +86 9318913515; fax: +86 9318912582.
E-mail address: yangzy@lzu.edu.cn (Z.-Y. Yang).

1386-1425/$ – see front matter © 2005 Elsevier B.V. All rights reserved.
doi:10.1016/j.saa.2005.05.007

derived and distilled by standard method. The rare earth(III) nitrates were derived from their oxide acquired from Nong Hua (PR China).

2.2. Physical measurements

The metal ions were determined by EDTA titration using xylenol oranges as an indicator. Carbon, nitrogen and hydrogen analyses were performed using a Vario EL elemental analyzer. Infrared spectra (4000–400 cm^{-1}) were obtained with KBr discs on a Therrno Mattson FTIR spectrometer. ^1H NMR spectra were recorded on a Varian Mercury Plus 300 BB, using TMS as an internal standard in DMSO-d_6. Mass spectra (fast atom bombardment) were recorded on a VG ZAB-HS mass spectrometer. Fluorescence measurements were made on a Hitachi RF-540 spectrofluorophotometer equipped with quartz cuvettes of 1 cm path length at room temperature. The molar conductance values measurements were carried out in DMF on a model DSS-11A conductivity meter.

2.3. Synthesis of ligand

The compounds of **1**–**4** (Fig. 1) were prepared according to the literature [5].

2.3.1. Preparation of *5*

An ethanol solution containing benzoyl hydrazine (1.36 g, 10 mmol) was added dropwise to another ethanol solution containing **4** (1.90 g, 10 mmol). The mixture was stirred for 2 h at room temperature and a white precipitate formed. The precipitate was collected by filtration and washed with ethanol. Recrystallization from 1:1 (v/v) DMF/H_2O gave the ligand, which was dried in a vacuum. Yield, 85%. M.P. 209–211 °C. ^1H NMR (DMSO-d_6, ppm): δ 11.95 (1H, br, NH), 10.18 (1H, s, OH), 8.79 (1H, s, 2-H), 8.65 (1H, s, CH=N), 7.95–7.25 (8H, m, Ph–H, 5,7,8-H). FAB MS: $m/z = 309$ (M + H).

Table 1
Crystal data and structure refinement for Sm(III) complex

Empirical formula	C_{72} H_{66} N_{14} O_{39} Sm_2
Formula weight	2052.09
T (K)	298(2)
Crystal system	Triclinic
Space group	P-1
a (Å)	11.037(4)
b (Å)	14.770(5)
c (Å)	15.032(7)
α (°)	60.583(4)
β (°)	75.528(7)
γ (°)	88.999(4)
V (Å^3)	2050.6(14)
Z	1
Reflections collected	10694
Independent reflections	7082 [R(int) = 0.0226]
Goodness-of-fit on F^2	1.009
Final R indices [$I > 2\sigma(I)$]	R1 = 0.0349, wR2 = 0.0786
Largest difference peak, hole/e Å^{-3}	1.141, −0.539

2.4. Synthesis of the complexes

The ligand (1 mmol, 0.308 g) and the $Ln(NO_3)_3{\cdot}6H_2O$ (0.5 mmol) were added to the ethanol (10 mL). The mixtures were stirred at 60 °C. After 5 min, the mixtures solution was filtrated to move reside and continued stirring for 24 h at room temperature. A white precipitated, the Ln(III) complex, was separated from the solution by suction filtration, purified by washing several times with ethanol, and dried for 24 h in a vacuum. All the complexes are white powers and stable in air, but the crystals of the solvated Sm(III) complex is a light yellow and recrystallized from CH_3OH with slow evaporation at room temperature.

2.5. X-ray crystallography

A light yellow crystal of Sm(III) complex (0.42 mm × 0.19 mm × 0.13 mm) was determined with a Bruker Smart-1000 CCD diffractometer by a graphite monochromatic

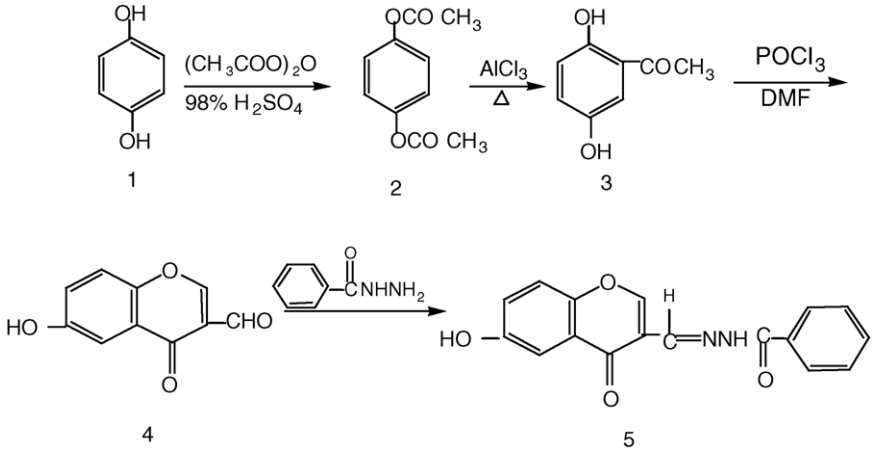

Fig. 1. Scheme of the synthesis of the ligand.

Mo Kα radiation (λ = 0.71073 Å) at 298(2) K. The crystallographic data are given in Table 1. The intensity data were collected by the ω scan mode within $2.14 < \theta < 25.03^\circ$ for *hkl* ($-13 \le h \le 12$, $-17 \le k \le 17$, $-17 \le l \le 17$). The structure was solved by direct method, the positions of rest non-hydrogen atoms were determined from successive Fourier syntheses, and the hydrogen atoms except water hydrogens were placed in the geometrically calculated positions. The positions and anisotropic thermal parameters of all non-hydrogen atoms were refined on F^2 by full-matrix least-squares techniques with SHELX-97 program package. Absorption correction was employed using semi-empirical from equivalents.

3. Result and discussion

3.1. Properties of the complexes

Analytical data for the complexes, presented in Table 2, conform to $Ln(NO_3)_3L_2$. All of the complexes are soluble in DMSO, DMF, methanol and methanol/chloroform (1:1), slightly soluble in ethanol, insoluble in benzene, water and diethyl ether, and may be kept in air for along time. Conductivity measurements for these complexes in DMF solution (Table 2) indicate that all complexes are 1:1 ionic compounds [6].

3.2. IR spectra

The IR spectra of the complexes are similar. Table 3 shows the characteristic bands of ligand and its complexes. The $\nu_{(carbony)}$ (C=O) and $\nu_{(hydrazonic)}$ (C=O) vibrations of the free ligand are at 1632 and 1649 cm^{-1}, respectively; for the complexes these peaks shift to 1609 and 1634 cm^{-1} or so, $\Delta\nu_{(ligand\text{-}complexes)}$ is equal to 23–33 and 12–15 cm^{-1}. The band at 591 cm^{-1} is assigned to ν (M–O). These demonstrate that the oxygen of carbonyl has formed a coordinative bond with the rare earth ions [7]. The band at 1598 cm^{-1} for the free ligand is assigned to the ν (C=N) stretch, which shifts to 1571–1573 cm^{-1} for its complexes. Weak bands at 427 cm^{-1} are assigned to ν (M–N). These further confirm that the nitrogen of the imino-group bonds to the rare earth ions [7]. The absorption bands of the coordinated nitrates were observed at about 1480 (ν_{as}) and 840 (ν_s) cm^{-1}. The ν_3 (E′) free nitrates appear at 1384 cm^{-1} in the spectra of the complexes [8], in agreement with the result of the conductivity experiments. In addition, the separation of the two highest frequency bands $|\nu_4 - \nu_1|$ is approximately 154 cm^{-1}, indicating that the coordinated nitrate groups in the complexes are bidentate.

3.3. Crystal structure of Sm(III) complex

The coordination of the hydrazone with lanthanide(III) results in the formation of five-membered (two SmN-NCO) and six-membered (two SmNOCCO) chelating rings in which the lanthanide ion is ten-coordinated. The complex **2** crystallized in a triclinic lattice with a space group *P*-1. Each unite cell contains two molecules. ORTEP drawing with the atoms numbering scheme for $[SmL_2(NO_3)_2]NO_3{\cdot}0.5H_2O{\cdot}2CH_3OH$ are shown in Fig. 2. In fact, the formula of Sm complex should be double molecule in the unit cell (Fig. 3). Main bond lengths and angles are summarized in Table 4. The coordination polyhedron for complex **2** is described by two nitrate group coordinated as bidentate, six donors atoms (four iminolic oxygen and two nitrogen) of the two ligands. There are five types of the coordination bonds in the complex **2**; its bond lengths are: Sm–O (hydrazonic) 2.476(3) and 2.510(3) Å, Sm–O (carbonyl) 2.438(3) and 2.367(3) Å, Sm–N (hydrazonic) 2.700(3) and 2.672(4) Å, Sm–O (nitrate) 2.499(3), 2.479(3), 2.574(3) and 2.570(3) Å. The Sm–O (carbony) distance (mean 2.402 Å) is significantly shorter than the Sm–O (hydrazonic) distance (mean 2.493 Å), which suggests that the Sm–O (carbony) bond is stronger

Table 2
Analytical and molar conductance data for the complexes

Complexes	C% found (calc.)	H% found (calc.)	N% found (calc.)	Ln% found (calc.)	Λ_m (s cm^2 mol^{-1})
1	42.94(42.77)	2.27(2.51)	10.86(10.27)	15.89(15.93)	92
2	42.46(42.86)	2.36(2.52)	10.78(10.29)	15.52(15.70)	121.8
3	42.20(42.46)	2.32(2.50)	10.09(10.20)	16.85(16.54)	102
4	42.67(42.30)	2.31(2.49)	9.89(10.16)	16.14(16.85)	104.8

Table 3
IR spectral data of the free ligands and its complexes (cm^{-1})

Compounds	$\nu_{(carbony)}$ (C=O)	$\nu_{(hydrazonic)}$ (C=O)	ν (C=N)	ν_1 (NO_3)	ν_2 (NO_3)	ν_3 (NO_3)	ν_4 (NO_3)	ν_0 (NO_3)	ν (M–O)	ν (M–N)
L	1632	1649	1598							
1	1609	1634	1573	1480	1187	840	1325	1383	596	426
2	1609	1636	1571	1480	1187	838	1325	1380	595	427
3	1609	1634	1572	1480	1187	840	1326	1384	591	427
4	1609	1637	1572	1480	1186	838	1325	1382	596	429

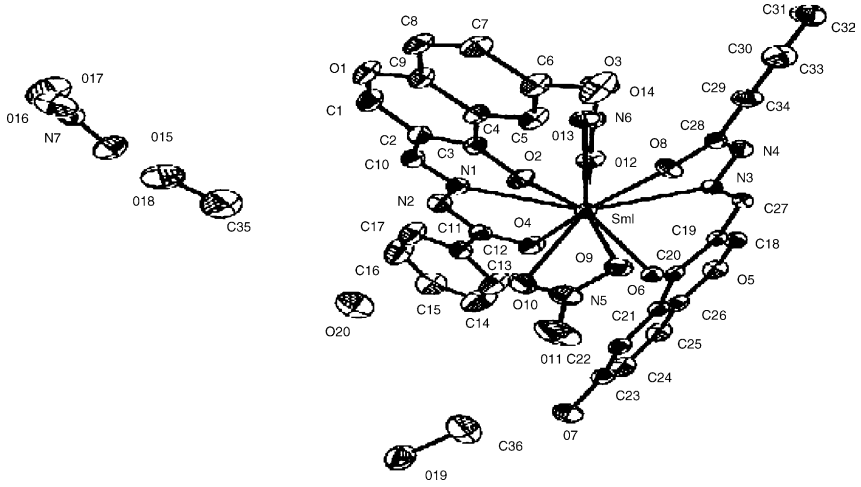

Fig. 2. ORTEP drawing of Sm(III) complex.

than the Sm–O (hydrazonic) bond, in agreement with the IR spectral data.

In complex the C_{11}–N_2 and C_{28}–N_4 distances are consistent with a double bond while the C_{11}–O_4 and C_{28}–O_{11} distances are consistent with a single bond.

3.4. Fluorescence studies

The fluorescence characteristics of the complexes in solid are listed in Table 5. The solid complexes have characteristic line emission of f–f transitions of metal ions when they are

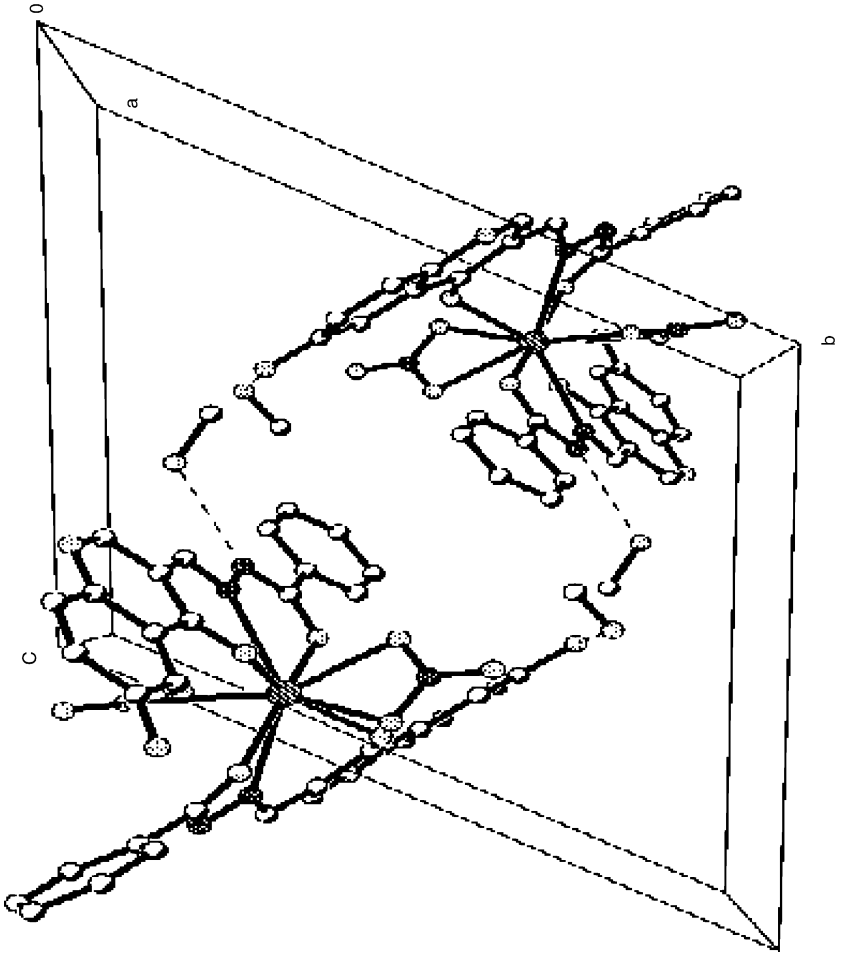

Fig. 3. Packing diagram in the unit cell showing hydrogen bonding.

Table 4
Select bond lengths (Å) and angles (°) for complex **2**

Sm(1)─O(2)	2.367(3)	Sm(1)─O(8)	116.37(11)	O(4)─Sm(1)─O(12)	66.68(11)
Sm(1)─O(6)	2.438(3)	Sm(1)─O(13)	68.63(10)	O(10)─Sm(1)─O(12)	139.79(11)
Sm(1)─O(4)	2.476(3)	Sm(1)─O(12)	73.21(10)	O(9)─Sm(1)─O(12)	163.22(10)
Sm(1)─O(10)	2.479(3)	Sm(1)─N(3)	2.510(3)	O(8)─Sm(1)─O(12)	103.72(10)
Sm(1)─O(9)	2.499(3)	Sm(1)─N(1)	2.570(3)	O(2)─Sm(1)─N(3)	127.26(10)
O(2)─Sm(1)─O(6)	148.36(9)	O(10)─Sm(1)─O(8)	2.574(3)	O(6)─Sm(1)─N(3)	64.73(9)
O(2)─Sm(1)─O(4)	122.91(11)	O(9)─Sm(1)─O(8)	2.672(4)	O(4)─Sm(1)─N(3)	106.59(11)
O(6)─Sm(1)─O(4)	67.70(9)	O(2)─Sm(1)─O(13)	2.700(3)	O(10)─Sm(1)─N(3)	138.25(11)
O(2)─Sm(1)─O(10)	76.94(11)	O(9)─Sm(1)─N(1)	124.39(10)	O(9)─Sm(1)─N(3)	97.73(10)
O(6)─Sm(1)─O(10)	78.37(11)	O(8)─Sm(1)─N(1)	128.22(10)	O(8)─Sm(1)─N(3)	59.43(10)
O(6)─Sm(1)─O(10)	78.37(11)	O(13)─Sm(1)─N(1)	73.31(11)	O(13)─Sm(1)─N(3)	74.60(10)
O(4)─Sm(1)─O(10)	74.36(12)	O(12)─Sm(1)─N(1)	72.25(10)	O(12)─Sm(1)─N(3)	65.93(10)
O(2)─Sm(1)─O(9)	75.99(10)	N(3)─Sm(1)─N(1)	137.65(10)	O(2)─Sm(1)─N(1)	66.97(10)
O(6)─Sm(1)─O(9)	73.18(10)	O(13)─Sm(1)─O(12)	49.07(10)	O(6)─Sm(1)─N(1)	127.32(10)
O(4)─Sm(1)─O(9)	117.59(10)	O(4)─Sm(1)─O(13)	109.06(10)	O(4)─Sm(1)─N(1)	60.30(10)
O(10)─Sm(1)─O(9)	51.13(11)	O(9)─Sm(1)─O(13)	132.80(10)	O(10)─Sm(1)─N(1)	80.34(11)
O(2)─Sm(1)─O(8)	70.06(11)	O(8)─Sm(1)─O(13)	67.68(10)	O(6)─Sm(1)─O(13)	135.07(9)
O(6)─Sm(1)─O(8)	104.40(10)	O(2)─Sm(1)─O(12)	116.35(10)	O(10)─Sm(1)─O(13)	145.99(11)
O(4)─Sm(1)─O(8)	165.96(10)	O(6)─Sm(1)─O(12)	95.28(9)		

Table 5
Fluorescence data of the complexes at room temperature

Complexes	State	Slit (nm)	λ_{ex} (nm)	λ_{em} (nm)	RFI[a]	Assignment
1	Solid	2.5	344	579.2	129.9	$^5D_0 \rightarrow {}^7F_0$
				591.6	829.8	$^5D_0 \rightarrow {}^7F_1$
				615.8	1818	$^5D_0 \rightarrow {}^7F_2$
2	Solid	2.5	333	562.4	37.96	$^4G_{5/2} \rightarrow {}^6H_{5/2}$
				594.6	45.71	$^4G_{5/2} \rightarrow {}^6H_{7/2}$
				641.0	12.34	$^4G_{5/2} \rightarrow {}^6H_{7/2}$

[a] RFI is relative fluorescence intensity.

excited with UV light. The solid complexes of Eu and Sm (Figs. 4 and 5) show strong fluorescence emission, and the fluorescence intensity of Eu(III) complexes is the strongest. Based on the theory of antenna effect [9,10], the intensity of the luminescence of Ln^{3+} complexes is related to the efficiency of the intramolecular energy transfer between the triple level of the ligand and the emitting level of the ions, which depends on the energy gap between the two levels. In the solid state, probably the energy gap between the ligands triplet levels and the emitting levels of the europium favor the energy transfer process for europium. This makes the europium complex show the most intense red fluorescence. However, the Dy and Tb(III) complexes do not exhibit fluorescence, which indicates that energy transfer process between the ligands triplet levels and the emitting levels of the Dy and Tb(III) does not favor.

The solid fluorescence emission peaks of Eu(III) complex are all from $^5D_0 \rightarrow {}^7F_J$ transition, and $^5D_0 \rightarrow {}^7F_2$

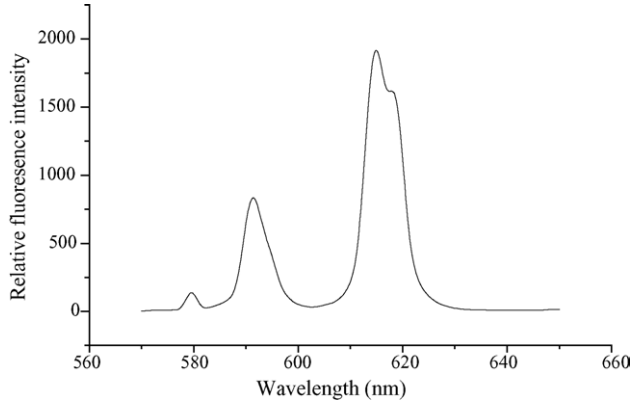

Fig. 4. The fluorescence emission spectra of the Eu(III) complex.

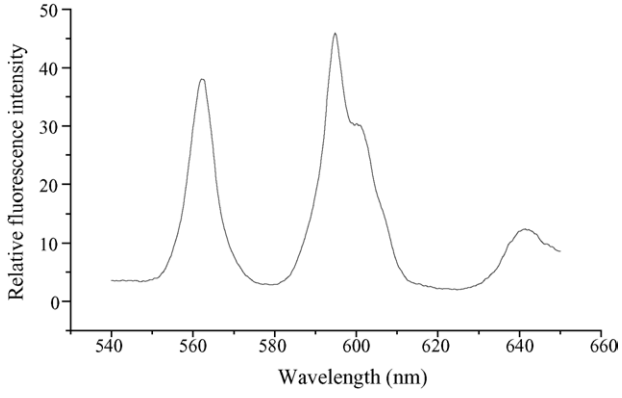

Fig. 5. The fluorescence emission spectra of the Sm(III) complex.

Table 6
Fluorescence data of the complex **1** at room temperature

Complex	Solve	Slit (nm)	λ_{ex} (nm)	λ_{em} (nm)	RFI[a]	Assignment
C_1	DMSO	5.0	394	591	11.3	$^5D_0 \rightarrow {}^7F_1$
				613	6.97	$^5D_0 \rightarrow {}^7F_2$
				650	0.66	$^5D_0 \rightarrow {}^7F_3$
				691	1.12	$^5D_0 \rightarrow {}^7F_4$
C_1	$CH_3OH/CHCl_3$	5.0	391	572	3.32	$^5D_0 \rightarrow {}^7F_0$
				591	4.61	$^5D_0 \rightarrow {}^7F_1$
				615	8.36	$^5D_0 \rightarrow {}^7F_2$
C_1	DMF	5.0	394	591	0.61	$^5D_0 \rightarrow {}^7F_1$
				616	0.84	$^5D_0 \rightarrow {}^7F_2$

C represents concentration: 5.0×10^{-4} mol L^{-1}.
[a] RFI is relative fluorescence intensity.

transition is an electric dipole transition. It can be detected as a relatively strong peak when Eu^{3+} does not lie in centrosymmetric ligand field. $^5D_0 \rightarrow {}^7F_1$ transition is a magnetic dipole transition, and its fluorescence intensity becomes the most intensive only when Eu^{3+} ion is center of inversion. In Tables 5 and 6, it can be seen that the intensity of $^5D_0 \rightarrow {}^7F_2$ transition is far stronger than that of $^5D_0 \rightarrow {}^7F_1$ in solid, DMF and $CH_3OH/CHCl_3$ (1:1, v/v), and a higher value for $\eta_{Eu} = {}^5D_0 \rightarrow {}^7F_2/{}^5D_0 \rightarrow {}^7F_1$ ($\eta_{Eu} = 2.19$ (solid), 1.38 (DMF) and 1.82 ($CH_3OH/CHCl_3$ (1:1, v/v)) indicates that the line-like emission spectra results from intra-4f transitions of predominantly electric dipole character, and thus Eu^{3+} lies in a non-centrosymmetric ligand field [11]. However, in the DMSO, a lower value for $\eta_{Eu} = {}^5D_0 \rightarrow {}^7F_2/{}^5D_0 \rightarrow {}^7F_1$ ($\eta_{Eu} = 0.62$) indicates that the line-like emission spectra results from intra-4f transitions of predominantly magnetic dipole character, and thus Eu^{3+} lies in a centrosymmetric ligand field. From the above discussion, we can draw a conclusion that the geometry of the complex has been changed by DMSO coordination.

The influence of solvent on the fluorescence intensities of the Eu(III) complex was investigated. As given in Table 6 and Fig. 6, the fluorescence intensities of the Eu(III) complex in organic solvent are weaker than that of powder. This may be due to the quench process of solvent molecules in the solution. The fluorescence intensity order of the Eu(III) complex (at the same concentration) in different solvents is DMSO > $CH_3OH/CHCl_3$ (1:1) > DMF. The fluorescence intensity measured in $CH_3OH/CHCl_3$ is lower than the one measured in DMSO because radiationless energy transfer competes with the radiative processes through coupling of the emissive states of Eu^{3+} ion to the O–H vibrational overstones. Besides, in DMF, which has a higher dielectric constant than $CH_3OH/CHCl_3$ (1:1), the europium complex exhibits the lowest intensity. This fact is due to the high coordination ability of DMF, whose oscillatory motions consume most of the energy transferred from the hydrazone to the metal ion.

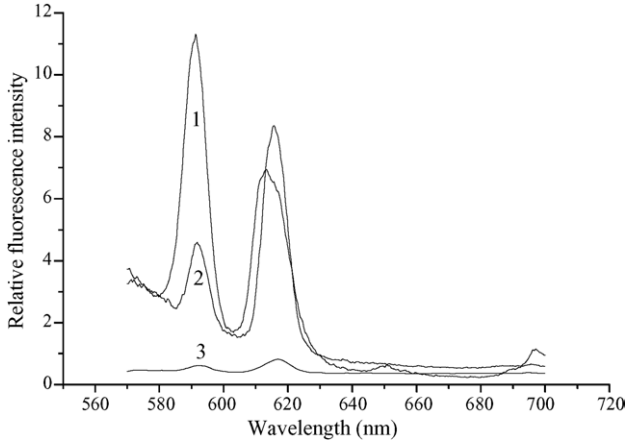

Fig. 6. The fluorescence emission spectra of the Eu(III) complex in DMSO (line 1), in $CH_3OH/CHCl_3$ (1:1, v/v) (line 2) and in DMF (line 3) solution at room temperature. Concentration: 5.0×10^{-4} mol L^{-1}.

We also see that the emission spectra of the Eu(III) complex exhibit different bands in different solvents. Interestingly, the Eu complex exhibits four bands in DMSO, corresponding to $^5D_0 \rightarrow {}^7F_1$, $^5D_0 \rightarrow {}^7F_2$, $^5D_0 \rightarrow {}^7F_3$ and $^5D_0 \rightarrow {}^7F_4$ transitions. Comparing to the fluorescence of solid complex, the $^5D_0 \rightarrow {}^7F$ and $^5D_0 \rightarrow {}^7F_4$ emission peaks were be observed at about 650 and 691 nm. These indicate that solvent molecules have strong coordination effect, and that the environment plays an important role in determining the fluorescence intensity of the complexes [12].

Acknowledgements

This work is supported by the National Natural Science Foundation of China (20475023) and Gansu NSF.

References

[1] G. Mathis, G. Clin, Chemistry (Washington, DC) 39 (1993) 1953.
[2] G.L. Denardo, G.R. Mirik, J. Nucl. Med. 37 (1996) 451.
[3] C. Galoup, C. Dicord, B. Cathala, Helv. Chem. Acta 82 (1999) 543.
[4] Y.X. Ceng, M.Q. Jin, H.W. Shu, Progress in Coordination Chemistry, vol. 8, Higher Education Press, Beijing, 2000, p. 17.
[5] J.X. Yu, F.M. Liu, W.J. Lu, Chin. J. Org. Chem. 20 (2000) 74.

[6] W.J. Greary, Coord. Chem. Rev. 7 (1971) 81.
[7] Y.Z. Yang, Synth. React. Inorg. Met.-Org. Chem. 30 (2000) 1269.
[8] Y. Hirashima, K. Kanetsuki, I. Yonezu, Bull. Chem. Soc. Jpn. 56 (1983) 738.
[9] J.-M. Lehn, Angew. Chem. Int. Ed. Engl. 29 (1990) 1304.
[10] M. Latva, H. Takalo, K. Simberg, J. Kankare, J. Chem. Soc. Perkin Trans. 2 (1995) 995.
[11] X. Hu, S. Cui, L. Yan, R.D. Yang, J. Rare Earths 21 (2003) 397.
[12] D.J. Zhou, Q. Li., C.H. Huang, G.Q. Yao, S. Umetani, M. Matsui, L.M. Ying, A.C. Yu, X.S. Zhao, Polyhedron 16 (1997) 1381.